Synthesis, Powder-Metallurgical Production and Lithium Tracer Diffusion in $LiNi_{0.33}Mn_{0.33}Co_{0.33}O_2$ Cathode Material for Lithium-Ion Batteries

D. Uxa, H. J. Holmes, L. Dörrer, H. Schmidt

AG Mikrokinetik, Institut für Metallurgie, Technische Universität Clausthal

K. Meyer

AG Energiewandlung, Institut für Energieforschung und Physikalische Technologien, Technische Universität Clausthal

daniel.uxa@tu-clausthal.de

Abstract

The $Li(Ni_{0.33}Mn_{0.33}Co_{0.33})O_2$ (NMC_{333}) compound is one of the most promising cathode materials for Li-ion batteries. In the following, the solid-state reaction in a two-step synthesis scheme of this material is examined, as well as the powder-metallurgical production of sintered bulk samples. Long range Li tracer self-diffusion is investigated in polycrystalline sintered bulk NMC_{333} samples with an average grain size of about 50 nm. For analysis, stable ^6Li tracers are used in combination with secondary ion mass spectrometry. At a temperature of T = 300 °C the determined Li diffusivity yields D_{Li} = $4.9 \cdot 10^{-16}$ m^2/s.

1 Introduction

Lithium-ion batteries (LIBs) are energy storage devices with a high energy density and widely applied as power sources for portable electronic devices (smart phones, laptops, tablets, navigation systems), in the field of transportation (HEVs, PHVs, EVs, pedelecs), and as miniaturized energy sources for future applications (smart cards, sensors, on-chip applications) [1–5]. Further improvements in energy density, power density and cycle stability are necessary, which require especially a fundamental understanding of kinetics that governs the lithiation mechanism of the electrode material. In this context, especially the Li diffusion is of high relevance. Li diffusion directly influences charging/discharging times, maximum capacities, electrode stability and possible side reactions [6].

Various types of cathode materials are in widespread commercial use today and comprehensive research on novel cathode materials is sought [7–9]. Most materials are based on lithium-metal-oxide compounds like $LiCoO_2$ (layered structure) (LCO), $LiMn_2O_4$ (spinel structure) (LMO) or $LiFePO_4$ (polyanion structure) [8]. Within the first LCO class the modified so-called NMC compounds $Li(Ni_{0.33}Mn_{0.33}Co_{0.33})O_2$, $Li(Ni_{0.5}Mn_{0.3}Co_{0.2})O_2$ and $Li(Ni_{0.8}Mn_{0.1}Co_{0.1})O_2$ are of relevance for applications as well for fundamental studies [10–12]. In this NMC class Co is partly replaced with Ni and Mn and solid solution behaviour is observed, while the material is structurally stable upon cycling.

The present work focuses on the synthesis and powder metallurgical production of the $LiNi_{0.33}Mn_{0.33}Co_{0.33}O_2$ (NMC_{333}) compound, which is one of the most promising cathode materials today, as well as on Li tracer diffusion. NMC_{333} can be synthesized from the starting materials Li_2CO_3, NiO, MnO_2 and Co_3O_4 using a solid-state reaction in a two-step scheme. Alternatively, commercial NMC_{333} starting material is used. In order to produce samples and sputter targets, the processed or commercial powder has to be pressed into cylindrical specimens and sintered, where the relative density of the material is of importance.

Long range and Li selective diffusion processes can be investigated very well by tracer methods (stable or radioactive) and adequate isotope depth profiling. Tracer methods give a direct measurement of the lithium tracer diffusion coefficient without relying on model-dependent correction factors. However, no experimental data from systematic Li tracer diffusion experiments on NMC_{333} cathode material is available to our best knowledge.

Here, we use rare stable isotopes of lithium: ^6Li with a natural abundance of 7.5 % and ^7Li with an abundance of 92.5 %, while ^6Li can be used as a tracer.

In this study we present a ^6Li based tracer experiment on a $LiNi_{0.33}Mn_{0.33}Co_{0.33}O_2$ (NMC_{333}) dense bulk sample using isotope heterostructures [13] and isotope depth profiling by Secondary Ion Mass Spectrometry (SIMS).

2 Experimental

Powder of $LiNi_{0.33}Mn_{0.33}Co_{0.33}O_2$ (NMC_{333}) composition was obtained from Sigma-Aldrich with a particle size less than 0.5 µm. Compacted pellets were prepared from the powder by pressing at various pressures from p = 100 to 475 MPa with steps of 75 MPa, forming cylindrical samples of 8 mm diameter. The pellets were sintered at

T = 800 °C in air either for t = 12 h or 24 h, preceded by heating at 3 K/min, and followed by cooling at the same rate, yielding 12 different sample types of NMC_{333} in total. In order to determine the relative element concentrations, the obtained NMC_{333} powder as well as the sintered samples were analysed by Inductively Coupled Plasma - Optical Emission Spectroscopy (ICP-OES) using a Plasma Quant 9100 (Analytik Jena, Germany). The dense pellets were polished for further use in diffusion experiments. Structural investigation of the bulk NMC_{333} samples was done by X-ray diffractometry measurements in θ/2θ mode after sintering using a Bruker D8 Discover diffractometer (CuK_α, 40 keV, 40 mA). Surface and microstructure of the sintered pellets were investigated using a Dualbeam SEM/FIB microscope (FEI Helios Nanolab 600) as well as a SEM microscope (CAMSCAN CS44). The sample density of 12 NMC_{333} samples was estimated from SEM micrographs using PxFworkbench software.

The tracer deposition for the diffusion experiments was done by sputtering a thin layer of ^6Li isotope enriched $LiNi_{0.33}Mn_{0.33}Co_{0.33}O_2$ (6-NMC_{333}) on top of the samples. Ion-beam sputtering was carried out using a commercial sputtering unit (IBC 681, Gatan) equipped with two penning ion sources. The deposition was done at 5 keV and at 200 µA using argon sputter gas at an operation pressure of $5 \cdot 10^{-3}$ mbar. The base pressure was better than $5 \cdot 10^{-7}$ mbar. A corresponding ^6Li-enriched sputter target was prepared by solid state syntheses using a two-step reaction route. This process is shown schematically in *Fig. 1*.

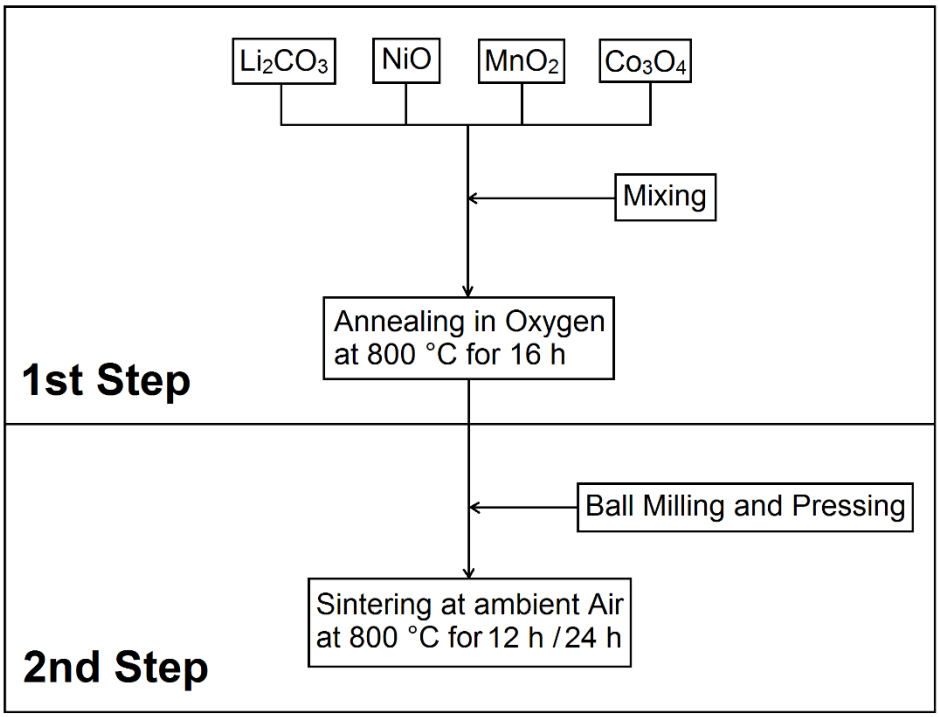

Fig. 1: Schematic representation of the $LiNi_{0.33}Mn_{0.33}Co_{0.33}O_2$ synthesis by means of a two-step solid-state reaction, which was used for preparing a ^{6}Li-enriched sputter target.

$^6Li_2CO_3$ (95 at-% ^{6}Li) powder was obtained from Sigma-Aldrich as well as NiO, Co_3O_4 and MnO_2 powder from Carl Roth. In the first step the starting materials were mixed in the corresponding stoichiometric ratio in an agate ball milling tank by adding an appropriate amount of ethanol in a ball mill (Wisd WiseMix Ball Mill) at 150 rpm for t = 1 h. The resulting black slurry was fully dried on a hot plate. The powder mixture was annealed at T = 800 °C with 3 K/min heating rate in pure oxygen for t = 16 h. After subsequent ball milling of the powder mixture (SPEX 8000M shaker mill) in the second step, a pellet of 2 cm diameter was pressed at p = 330 MPa and sintered at T = 800 °C in air for t = 12 h, preceded by heating at 3 K/min, and followed by cooling at the same rate, which yielded a polycrystalline dense sputter target.

Due to the fact that the ^{6}Li tracer layer and the dense samples have approximately the same chemical composition with regards to the lithium content, equilibrium isotope mixing is expected to be measured during the diffusion experiment. For the diffusion experiment the prepared NMC_{333} sample was annealed in air at the temperature of T = 300 °C for t = 10 min using a commercial rapid annealing setup (AO 500, MBE, Germany).

Depth profiles of the two Li isotopes and of Ni, Mn and Co were obtained by SIMS using a Cameca ims 3f/4f machine with O^- primary ions.

Analysis of the resulting sputter crater was performed by a stylus profilometer (Tencor Alphastep 500). In depth profile mode the primary beam is rastered over the surface (250 µm · 250 µm) and secondary ion signals are recorded as a function of sputter depth perpendicular to the surface. The relative ^{7}Li isotope fraction, c, is calculated from the ^{6}Li and ^{7}Li signal intensities I as measured by SIMS to:

$$c = \frac{I\left(^7\mathrm{Li}\right)}{I\left(^6\mathrm{Li}\right) + I\left(^7\mathrm{Li}\right)}. \quad (1)$$

3 Results and Discussion

The results of the ICP-OES analysis of the obtained commercial NMC_{333} powder as well as of a sintered NMC_{333} sample are listed in *Tab. 1*. The results, which are nearly identical for powder and the sintered sample, show a composition of $Li_{0.90}(Ni_{0.30}Mn_{0.39}Co_{0.32})O_{2.08}$ and indicate no loss of lithium during the sintering process. The oxygen concentration is slightly above the stoichiometric composition, and the Mn concentration is slightly higher compared to the other transition metals. Most importantly the lithium to metal ratio of 0.9 is lower by about 10 %, indicating slightly sub-stoichiometric samples, which is due to the commercial starting material.

Tab. 1: Relative element concentrations as analysed by ICP-OES of the as-received NMC_{333} powder and sintered samples under investigation.

	Li (at.-%)	Ni (at.-%)	Mn (at.-%)	Co (at.-%)	O (at.-%)
Powder	22.50 ± 0.1	7.49 ± 0.02	9.80 ± 0.06	8.15 ± 0.04	52.06 ± 0.21
Sample	22.50 ± 0.1	7.42 ± 0.02	9.88 ± 0.06	8.05 ± 0.04	52.15 ± 0.21

The X-ray diffraction pattern of a sintered sample from commercial NMC_{333} powder is shown in *Fig. 2*. All Bragg peaks belong to the hexagonal α-$NaFeO_2$-type layered structure. Unknown Bragg peaks are not observed. The lattice parameters are a = 2.863(2) Å and c = 14.228(3) Å in good agreement to stoichiometric NMC as shown in ref. [14]. Using the Scherrer formula on the different peaks the crystallites size can be assessed to about 50 nm, indicating a nano-crystalline structure.

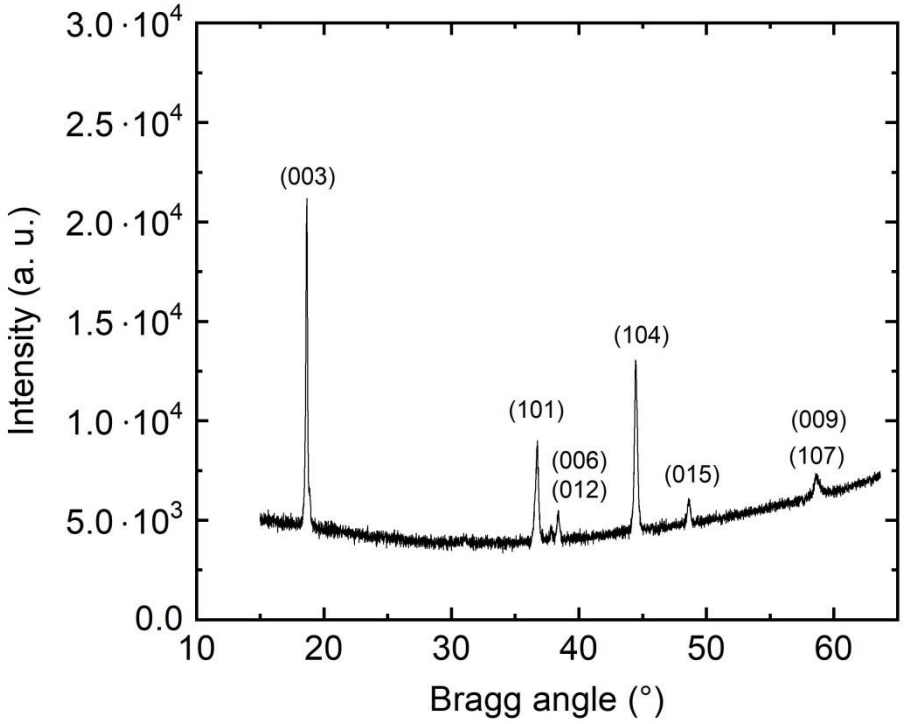

Fig. 2: X-ray diffraction pattern of the bulk NMC_{333} sample sintered from commercial NMC_{333} powder.

To investigate the achievable density, samples were produced at six different pressures. The pressure varies from p = 100 to 475 MPa with a step size of 75 MPa. These pellets are sintered in ambient air at a temperature of T = 800 °C for a duration of t = 12 h or t = 24 h. This results in 12 different types of samples to be examined. The sample density of the 12 NMC_{333} sample types was estimated from SEM micrographs using PxFworkbench software with the help of a cross grid consisting of thousand points. The porous areas can be marked and counted. Ten SEM images of each sample are examined for their porosity and an average value is determined. In *Fig. 3* the relative density is plotted against the pressure used. It can be seen that the relative density varies in the range from 95.63% to 97.64%. Furthermore, no significant dependence on the pressing pressure used can be seen. One possible explanation for this is that the lowest value of the pressure of 100 MPa already enables the maximum relative density. The different sintering times of t = 12 h and t = 24 h also have no recognizable systematic influence.

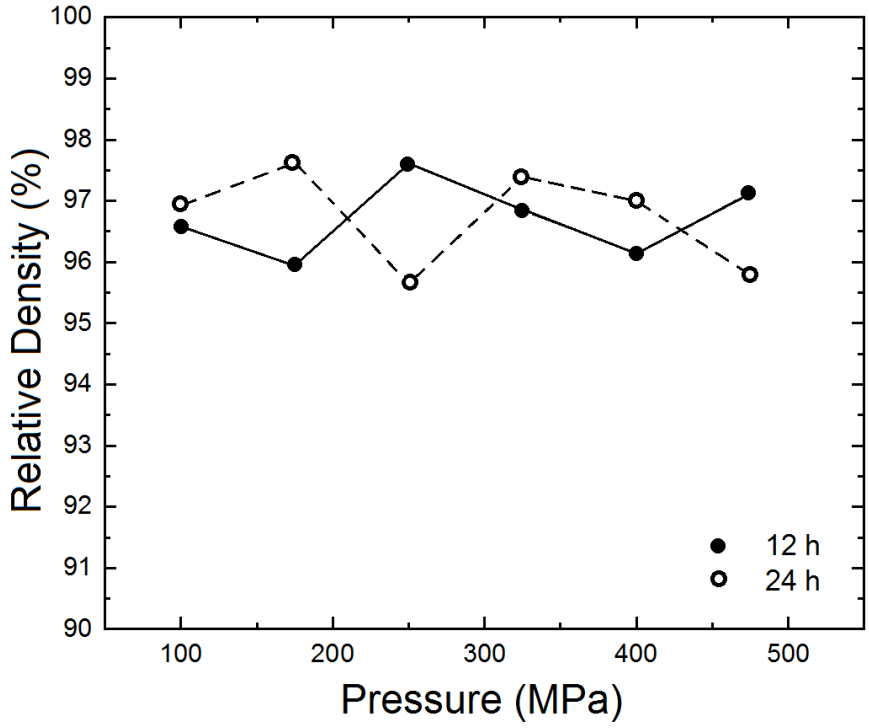

Fig. 3: Relative density plotted against the applied pressure for a sintering time of t = 12 h (solid lines) and 24 h (dotted lines).

A SEM image of a NMC_{333} bulk sample from commercial starting material that was pressed at p = 100 MPa and sintered for t = 12 h in ambient air at T = 800 °C is shown in *Fig. 4*. It can be seen that agglomerates of densely sintered particles have grown during sintering, much larger than the particle size of the as-received NMC_{333} powder. This shows that the result regarding the relative density of the samples with no significant open porosity can be achieved already with a pressure of p = 100 MPa. In order to map an effect of the pressure on the porosity of the samples, further investigations have to be carried out with significantly lower pressing pressures of p <100 MPa.

A noticeable feature of the pressed samples is the appearance of cracks (not shown here). While the pellets pressed at p = 100 MPa are very dense, all pellets that were pressed with p = 175 MPa or more pressure show cracks. This effect can be determined after t = 12 h and after t = 24 h of sintering. More cracks occur with increasing pressure. This was also noticeable during the pressing process, since it became increasingly difficult to obtain stable pellets.

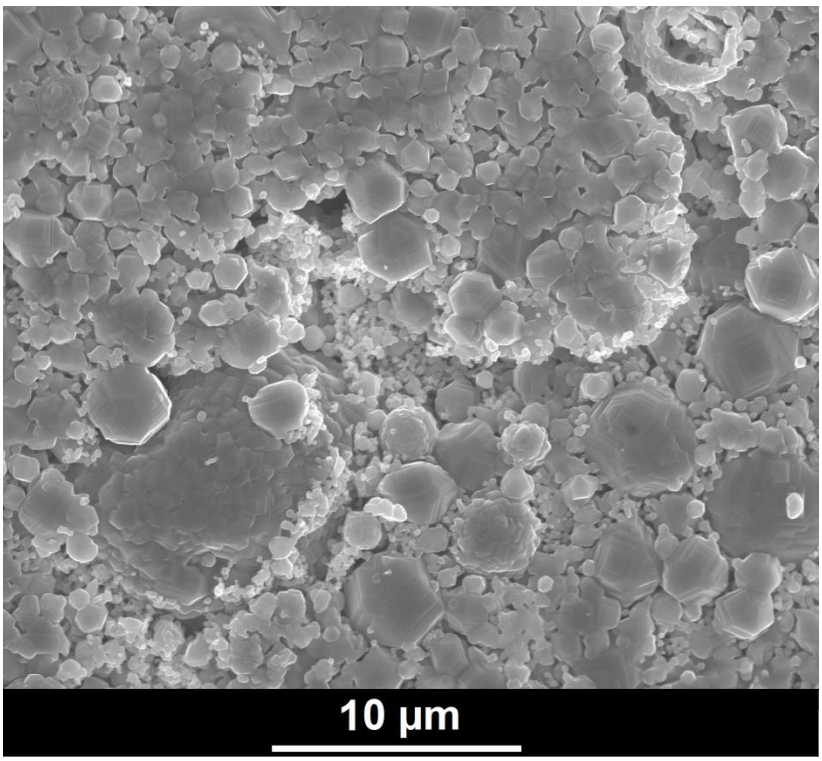

Fig. 4: SEM image of a NMC_{333} bulk sample which was pressed at p = 100 MPa and sintered for t = 12 h in ambient air at T = 800 °C.

In *Fig. 5* a SEM image of a cross-section of a two-step synthesized NMC_{333} bulk sample is shown, which was fabricated in the same way and with the same parameters as for the ^{6}Li isotope enriched $LiNi_{0.33}Mn_{0.33}Co_{0.33}O_2$ (6-NMC_{333}) sputter target. Here, particles are marked with different shades of gray. At the first marking point, a particularly dark particle is analyzed which, according to the results of the EDX analysis, is rich in manganese at 17.95 at.-%. At points two and four, particles with a medium gray level are analyzed. These have a high cobalt content, which in this analysis is between 21.37 at.-% and 24.06 at.-%. The light gray particles, one of which is examined in the third marking point, have a high nickel content of 37.07 at.-%. This inhomogeneity is an indication of insufficient mixing and that the solid-state reaction of the starting materials Li_2CO_3, NiO, Co_3O_4 and MnO_2 to the NMC_{333} composition has not been completed. Necessary extensions of the two-step synthetic route have to be discussed, e. g. repeating the second step of ball milling, mixing and sintering for several times. With regards to the sputter target used this inhomogeneity is less of a problem since the sputtering process is reactive.

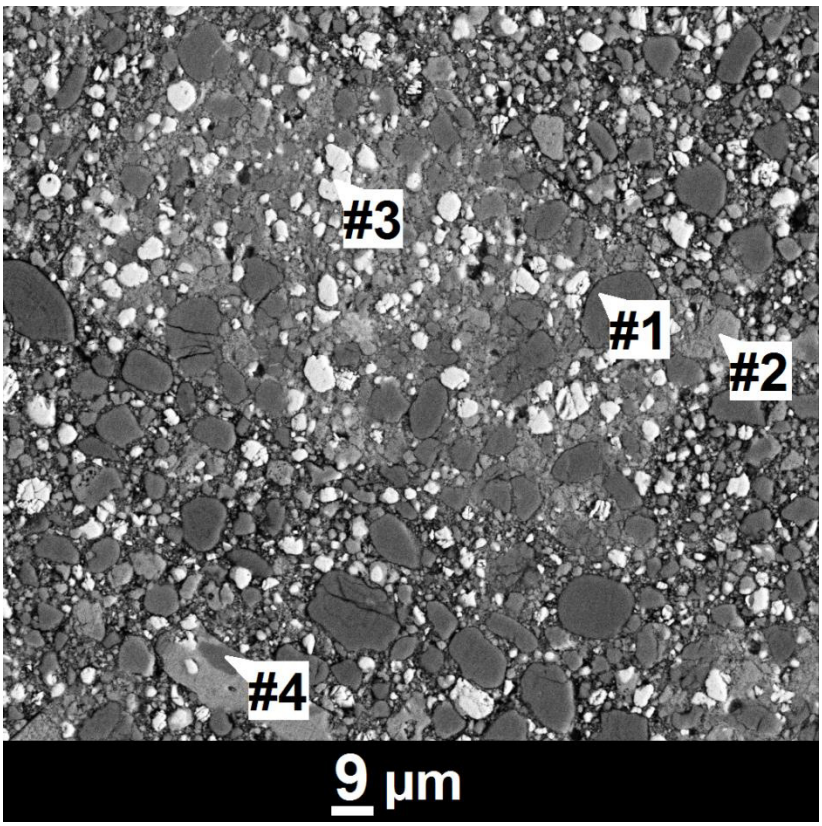

Fig. 5: SEM image of a cross-section of a two-step synthesized NMC_{333} sample, which was fabricated in the same way and with the same parameters as for the ^{6}Li isotope enriched $LiNi_{0.33}Mn_{0.33}Co_{0.33}O_2$ (6-NMC_{333}) sputter target. EDX analysis shows that #1 is enriched with Mn (17.95 at.-% Mn), #2 and #4 are enriched with Co (24.06 at.-% Co and 21.37 at.-% Co) and #3 is enriched with Ni (37.07 at.-% Ni).

ICP-OES analysis was also done for the two-step synthesized ^{6}Li isotope enriched $LiNi_{0.33}Mn_{0.33}Co_{0.33}O_2$ (6-NMC_{333}). The results are listed in *Tab. 2* and show a composition of $Li_{0.99}(Ni_{0.32}Mn_{0.32}Co_{0.35})O_{2.07}$. In contrast to the NMC_{333} samples fabricated from commercial powder the lithium to metal ratio is 0.99, close to the stoichiometric composition. If such a sputter target is used to produce a tracer layer by ion-beam sputtering, Li losses occur during the sputtering process [15]. Consequently, the resulting lithium to metal ratio in the tracer layer is expected to be close to 0.9.

Tab. 2: Relative element concentrations as analysed by ICP-OES of the two-step synthesized 6-NMC_{333} sputter target.

	Li (at.-%)	Ni (at.-%)	Mn (at.-%)	Co (at.-%)	O (at.-%)
6-NMC_{333}	23.99 ± 0.1	7.79 ± 0.02	7.85 ± 0.06	8.65 ± 0.04	51.71 ± 0.21

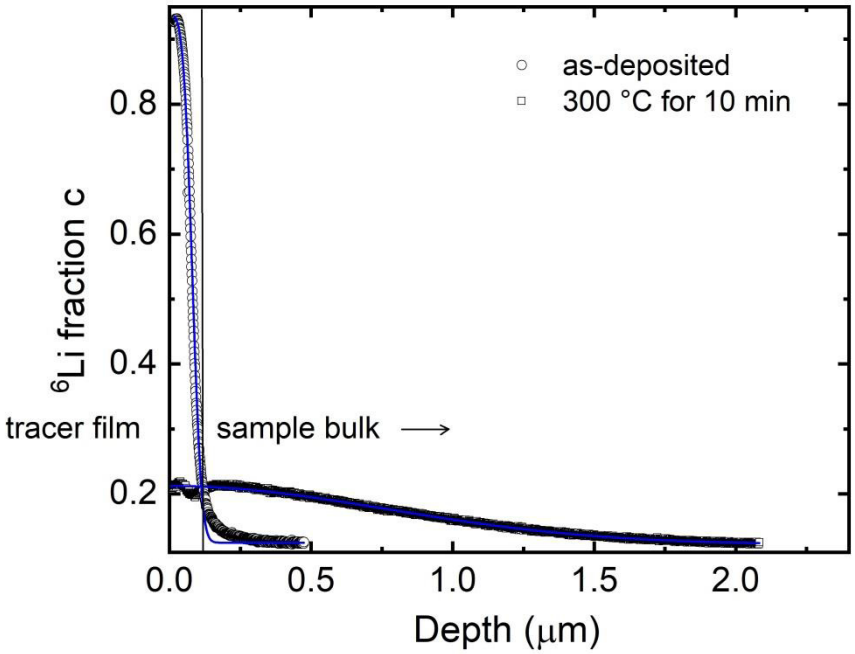

Fig. 6: Atomic fraction of ^{6}Li as a function of depth for an as-deposited sample and for a sample annealed at T = 300 °C for t = 10 min. Also shown are fitting curves according to equation (2) as solid lines.

Figure 6 shows characteristic SIMS depth profiles after ^{6}Li tracer deposition and after diffusion annealing at a temperature of T = 300 °C for t = 10 min in samples from as-received commercial powder with the composition of $Li_{0.90}(Ni_{0.30}Mn_{0.39}Co_{0.32})O_{2.08}$.. The relative ^{6}Li concentration, c, is plotted as a function of sputter depth. Without any diffusion annealing the depth profile can be fitted using the thick film solution to Fick's second law pertaining to diffusion across an interface:

$$c(x,t) = c_\infty + \frac{(c_0 - c_\infty)}{2}\left[\mathrm{erf}\left(\frac{h+x}{R}\right) + \mathrm{erf}\left(\frac{h-x}{R}\right)\right] . \qquad (2)$$

with $c_\infty = 0.12$ being the residual ^{6}Li concentration in the NMC_{333} bulk sample, $c_0 = 0.94$ being the ^{6}Li concentration present in the top 6-NMC_{333} layer, $h = 80.6$ nm the thickness of the ^{6}Li enriched layer and R = (35.9 ± 0.5) nm is the broadening of the lithium distribution at the interface.

Annealing leads to diffusion of the ^{6}Li tracer into the sample bulk connected with a noticeably broadening of the lithium distribution. The diffusion annealed sample was also fitted by equation (2) in order to determine the lithium tracer diffusivity. In this context, c_∞, c_0 and R are free fit parameters and h is fixed to the initial value.

The Li diffusivity D is determined from the difference in the respective broadening R of the lithium distribution of the diffusion profile and of the as-deposited profile, R_0, according to $D = (R^2 - R_0^2)/4t$, where t is the annealing time. The result is displayed as a continuous blue line in Fig. 6 with $D_{Li} = 4.9 \cdot 10^{-16}$ m^2/s.

It is known that the observable lithium diffusivity D_{Li} and the lithium vacancy diffusion coefficient D_{VLi} (termed defect diffusion coefficient) are related by the vacancy fraction x_{VLi}:

$$D_{Li} = x_{V_{Li}} D_{V_{Li}} \quad . \tag{3}$$

Therefore, the change of x in $Li_xNi_{0.33}Mn_{0.33}Co_{0.33}O_2$ to values higher or lower than x = 0.9 should correspond to a change of the measured Li diffusivity. Such experiments are in preparation and will be done together with measurements of Li diffusivity in the established $LiCoO_2$ cathode material, which enables a comparison of Li diffusivity in LCO and NMC_{333}.

4 Conclusion

A two-step solid-state synthesis is applied to produce ^{6}Li enriched $Li_{0.99}(Ni_{0.32}Mn_{0.32}Co_{0.35})O_{2.07}$ (6-NMC_{333}) which is used as a sputter target for lithium isotope tracer deposition. The lithium to metal ratio approximates the target value of one. The EDX analysis shows an inhomogeneous distribution of the metal oxides used, which suggests an incomplete reaction and insufficient mixing. Necessary extensions of the two-step synthetic route have to be discussed, e. g. repeating the second step of ball milling, mixing and sintering for several times. With the investigation of NMC_{333} sintered samples produced from commercial NMC_{333} powder we could show that the relative density achieved varies in the range from 95.63% to 97.64%, and no increase in

the relative density could be determined with increasing pressing pressure. Increasing the sintering time from 12 to 24 hours did not result in an increase in the relative density, too. The lowest pressure of p = 100 MPa is already sufficient and the maximum achievable relative density is already present. During sintering, agglomerates of densely sintered particles have grown, much larger than the particle size of the as-received NMC_{333} powder. The crystallites size can be assessed by XRD measurement to about 50 nm, indicating a nano-crystalline structure. Long range Li tracer self-diffusion is investigated in these sintered bulk NMC_{333} samples with a composition of $Li_{0.90}(Ni_{0.30}Mn_{0.39}Co_{0.32})O_{2.08}$ at a temperature of $T = 300$ °C and the determined Li diffusivity yields $D_{Li} = 4.9 \cdot 10^{-16}$ m^2/s.

Ackknowledgements

Financial support from the Deutsche Forschungsgemeinschaft (DFG) (Schm 1569/33-1) is gratefully acknowledged. We are indebted to G. Zander for ICP-OES analysis and helpful discussions, to Dr. R. Gustus and S. Lenk for SEM measurements, to J. Himmelstoß for technical assistance with the sputter deposition and to S. Fischer for carefully preparing the samples.

References

[1] Korthauer, R., Ed. Handbook Lithium-Ion Batteries, 1st ed. 2017; Springer Berlin; Springer Vieweg: Berlin, 2017.

[2] Julien, C.; Mauger, A.; Vijh, A. *Lithium batteries: Science and technology*, 2016.

[3] Etacheri, V.; Marom, R.; Elazari, R.; Salitra, G.; Aurbach, D. Challenges in the development of advanced Li-ion batteries: A review. Energy Environ. Sci. 2011, 4, 3243–3262.

[4] Aifantis, K. E., Ed. High energy density lithium batteries: Materials, engineering, applications; Wiley-VCH-Verl.: Weinheim, 2010.

[5] Bruce, P. G.; Scrosati, B.; Tarascon, J.-M. Nanomaterials for rechargeable lithium batteries. Angewandte Chemie (International ed. in English) **2008**, 47, 2930–2946.

[6] Soni, S. K.; Sheldon, B. W.; Xiao, X.; Bower, A. F.; Verbrugge, M. W. Diffusion Mediated Lithiation Stresses in Si Thin Film Electrodes. J. Electrochem. Soc. 2012, 159, A1520-A1527.

[7] George E. Blomgren. The Development and Future of Lithium Ion Batteries. J. Electrochem. Soc. 2016, 164, A5019.

[8] Chen, R.; Zhao, T.; Zhang, X.; Li, L.; Wu, F. Advanced cathode materials for lithium-ion batteries using nanoarchitectonics. Nanoscale horizons 2016, 1, 423–444.

[9] Xu, J.; Dou, S.; Liu, H.; Dai, L. Cathode materials for next generation lithium ion batteries. Nano Energy 2013, 2, 439–442.

[10] Zheng Li; Natasha A. Chernova; Megan Roppolo; Shailesh Upreti; Cole Petersburg; Faisal M. Alamgir; M. Stanley Whittingham. Comparative Study of the Capacity and Rate Capability of LiNi y Mn y Co1–2y O2 (y = 0.5, 0.45, 0.4, 0.33). J. Electrochem. Soc. 2011, 158, A516.

[11] Kim, M.-H.; Shin, H.-S.; Shin, D.; Sun, Y.-K. Synthesis and electrochemical properties of Li[Ni0.8Co0.1Mn0.1]O2 and Li[Ni0.8Co0.2]O2 via co-precipitation. Journal of Power Sources 2006, 159, 1328–1333.

[12] Wu, F.; Wang, M.; Su, Y.; Bao, L.; Chen, S. Surface of LiCo1/3Ni1/3Mn1/3O2 modified by CeO2-coating. Electrochimica Acta 2009, 54, 6803–6807.

[13] Rahn, J.; Hüger, E.; Dörrer, L.; Ruprecht, B.; Heitjans, P.; Schmidt, H. Li self-diffusion in lithium niobate single crystals at low temperatures. Phys. Chem. Chem. Phys. 2012, 14, 2427.

[14] Yin, S.-C.; Rho, Y.-H.; Swainson, I.; Nazar, L. F. X-ray/Neutron Diffraction and Electrochemical Studies of Lithium De/Re-Intercalation in Li 1-x Co 1/3 Ni 1/3 Mn 1/3 O 2 (x = 0 → 1). Chem. Mater. 2006, 18, 1901–1910.

[15] Schwab, C.; Höweling, A.; Windmüller, A.; Gonzalez-Julian, J.; Möller, S.; Binder, J. R.; Uhlenbruck, S.; Guillon, O.; Martin, M. Bulk and grain boundary Li-diffusion in dense $LiMn_2O_4$ pellets by means of isotope exchange and ToF-SIMS analysis. Phys. Chem. Chem. Phys. 2019, 21, 26066.

Autorenanschriften

M. Sc. Daniel Uxa

B. Sc. Helen J. Holmes

Dr. rer. nat. Lars Dörrer

Prof. Dr. rer. nat. Harald Schmidt

Technische Universität Clausthal

Institut für Metallurgie

AG Thermochemie und Mikrokinetik

Robert-Koch-Straße 42

38678 Clausthal-Zellerfeld

M. Sc. Kevin Meyer

Technische Universität Clausthal

Institut für Energieforschung und physikalische Technologien

AG Energiewandlung

Robert-Koch-Straße 42

38678 Clausthal-Zellerfeld